SAND2019-7444J

Correlation of Sensitive Volumes Associated with Ion- and Laser-Induced Charge Collection in an Epitaxial Silicon Diode

Kaitlyn L. Ryder, *Student Member, IEEE*, Landen D. Ryder, *Student Member, IEEE*, Andrew L. Sternberg, *Member, IEEE*, John A. Kozub, Enxia Zhang, *Senior Member, IEEE*, Ani Khachatrian, *Member, IEEE*, Steven P. Buchner, Dale P. McMorrow *Fellow, IEEE,* Joel M. Hales, *Member, IEEE*, Yuanfu Zhao, Liang Wang, Chuanmin Wang, Robert A. Weller, *Senior Member*, *IEEE,* Ronald D. Schrimpf, *Fellow, IEEE*, Sharon M. Weiss, *Member, IEEE*, and Robert A. Reed, *Fellow, IEEE*

***Abstract*—A sensitive volume is developed using pulsed laser-induced collected charge for two bias conditions in an epitaxial silicon diode. These sensitive volumes show good agreement with experimental laser-induced collected charge at a variety of focal positions and pulse energies. When compared to ion-induced collected charge, the laser-based sensitive volume over predicts the experimental collected charge at low bias and agrees at high bias. A sensitive volume based on ion-induced collected charge adequately describes the ion experimental results at both biases. Differences in the amount of potential modulation explain the differences between the ion- and laser-based sensitive volumes at the lower bias. Truncation of potential modulation by the highly doped substrate at the higher bias results in similar sensitive volumes.**

***Index Terms*— Pulsed laser, single-event effects, single-event transients, sensitive volume, two-photon absorption**

I. Introduction

THE single-event-effects (SEE) sensitive volume model was first defined in [1] in order to relate the energy deposited in a sensitive volume by an ionizing radiation event to a circuit response. In order to enable on-orbit estimation of single event effects rates, various versions of the sensitive volume model have been developed and used successfully. Early versions of the sensitive volume model defined the sensitive volume geometry as a rectangular parallelepiped (RPP) [1], [2]. Recent methods define a more complex sensitive volume geometry [3], [4] utilizing nested RPPs with varying collection efficiencies. Experimentally-determined sensitive volumes are often used as inputs to error rate calculation simulators such as the CRÈME96 tool [5], [6], [7] and MRED [3], [4]. The sensitive volumes are typically found using experimental data gathered at ground-based ion testing facilities.

Pulsed laser SEE testing is useful because of the refined spatial and temporal control of charge generation within devices, while offering increased availability and affordability compared to traditional ion beams [8], [9]. Recent research provides a theoretical and computational framework for quantitatively predicting pulsed laser SEE results [10], [11], empirical correlation of laser and ion results [12], [13], and a laser equivalent LET approach to correlate charge generated from pulsed lasers and ions [14]. However, it would be useful to develop a quantitative, predictive relationship between ion- and pulsed laser-induced SEEs without first empirically correlating laser and ion responses. A key, enabling metric towards this goal would be to define a common geometry for the sensitive volume generally useful for both ion- and laser-induced charge collection estimates.

In this work, a large area Si diode fabricated on an epi-layer is used to study the correlation between sensitive volume geometries defined by measurements of ion- and pulsed laser-induced collected charge. A common RPP sensitive volume thickness is determined from laser-induced collected

Manuscript submitted on July 4, 2019.

This work was supported in part by the Defense Threat Reduction Agency through its Basic Research program grant HDTRA1-16-1-0007 and Sandia National Lab's LDRD program.

Sandia National Laboratories is a multimission laboratory managed and operated by National Technology and Engineering Solutions of Sandia, LLC., a wholly owned subsidiary of Honeywell International, Inc., for the U.S. Department of Energy's National Nuclear Security Administration under contract DE-NA-0003525. This paper describes objective technical results and analysis. Any subjective views or opinions that might be expressed in the paper do not necessarily represent the views of the U.S. Department of Energy or the United States Government.

K. L. Ryder, L. D. Ryder, A. L. Sternberg, E. Zhang, R. A. Weller, R. D. Schrimpf, S. M. Weiss, and R. A. Reed are with the Department of Electrical Engineering and Computer Science, Vanderbilt University, Nashville, TN 37235 USA (e-mail: kaitlyn.h.ryder@vanderbilt.edu).

J. A. Kozub is with the Department of Physics and Astronomy, Vanderbilt University, Nashville, TN 37235 USA (e-mail: john.kozub@vanderbilt.edu).

A. Khachatrian, S. P. Buchner, D. P. McMorrow, and J. M. Hales are with U.S. Naval Research Lab, Washington, DC 37235 USA (e-mail: dale.mcmorrow@nrl.navy.mil).

J. M. Hales is with KeyW Corporation, Herndon, VA 20171 USA (e-mail: joelmh@hotmail.com).

A. Khachatrian, S. P. Buchner, D. P. McMorrow, and J. M. Hales are with Beijing Microelectronics Technology Institute, Beijin 100076 China (e-mail: wangliang150200@163.com).

charge measurements combined with optical simulations of laser-induced charge distribution profiles at different pulse energies and bias conditions. This sensitive volume geometry is combined with ion LET curves to predict collected charge from heavy ion experiments and compared to a sensitive volume defined from ion-induced collected charge. Despite the laser-defined sensitive volume exhibiting good agreement with laser-induced collected charge under a variety of conditions, it only shows agreement with ion-induced collected charge under particular bias conditions. The physical mechanisms responsible for the differences are discussed and limitations of quantitative ion-laser SEE measurements are considered.

II. Experimental Setup

An epitaxial Si diode manufactured by Beijing Microelectronics Technology Institute (BMTI) was used as a test structure in this work. A cross section of the diode can be seen in Fig. 1. The devices were manufactured with 154 μm^2 holes in the top Al metal contact, allowing for top-side illumination of the junction. The area of the metal holes accounts for less than 0.1% of the total area of the top contact, so electrical performance is not affected by the presence of the holes. The holes in the metallization are small enough to perturb the laser profile as it passes through it, so effects resulting from the optical perturbations are accounted for in the optical simulations when estimating the charge generated by the laser pulse.

A detailed description of the measurement setup can be found in [15], [16]. Ion testing was performed at Lawrence Berkeley National Lab's (LBNL) 88" Cyclotron using the 10 MeV/u cocktail. The list of ions used is shown in Table I [17]. The diode was biased at -5 V and -90 V for all experiments, resulting in depletion region widths of roughly 4 μm and 15 μm, respectively. A stainless steel pinhole 200 μm in diameter and 100 μm thick was used to isolate ion events to a small area of the active region of the diode, eliminating charge collection produced by ion events outside of the active diode region.

Pulsed laser testing was performed at the Naval Research Laboratory (NRL) Ultrafast Laser Facility [18] using two-photon absorption (TPA) at a wavelength of 1260 nm, and pulse energies of 450 pJ, 750 pJ, and 990 pJ. The FWHM spot size and temporal width of the laser pulse were 1.36 μm and 130 fs, respectively. A series of measurements made by changing the depth of the laser focus within a device, called a depth scan, was performed.

Optical simulations of the laser-induced charge generation profiles were done using Lumerical, an FDTD (finite difference time domain) nanophotonic simulation software package [19] (described in more detail later). Fig. 2 shows the time-integrated charge distribution profile from Lumerical for this particular laser setup at a focal position of 17.5 μm. A focal position of 0 μm corresponds to the laser being focused on the surface of the silicon, and positive focal positions correspond to the laser being focused within the silicon.

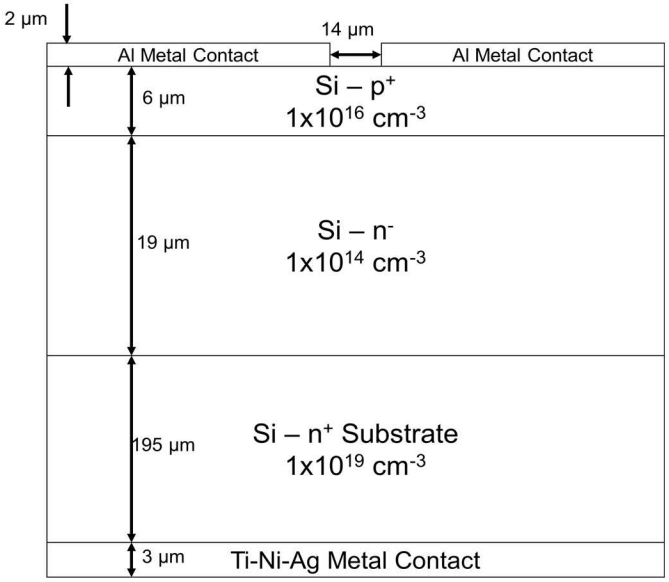

Fig. 2. Cross-section of BMTI epitaxial silicon diode. The diode is 2.25 mm^2 and 220 μm think. The *pn* junction occurs roughly 6 μm into the silicon, the epi-layer is approximately 19 um think, and the substrate starts approximately 25 μm into the silicon. There are 154 μm^2 holes in the top metal contact, allowing for topside illumination.

III. Laser-Induced Collected Charge Results

Lumerical FDTD Solutions is a nanophotonic simulation tool that captures optical and nanophotonic effects through a three-dimensional solution of Maxwell's Equations. It has been modified to account for charge generation from various nonlinear effects associated with the Kerr effects, free-carrier refraction and absorption, and TPA [20], an approach similar to

TABLE I
LBNL Ions

Ion	Energy (MeV)	Surface Incident LET (MeV-cm^2/mg)	Range in Si (μm)
Xe	1230	59	90.0
Cu	660	21	108
Si	290	6	142

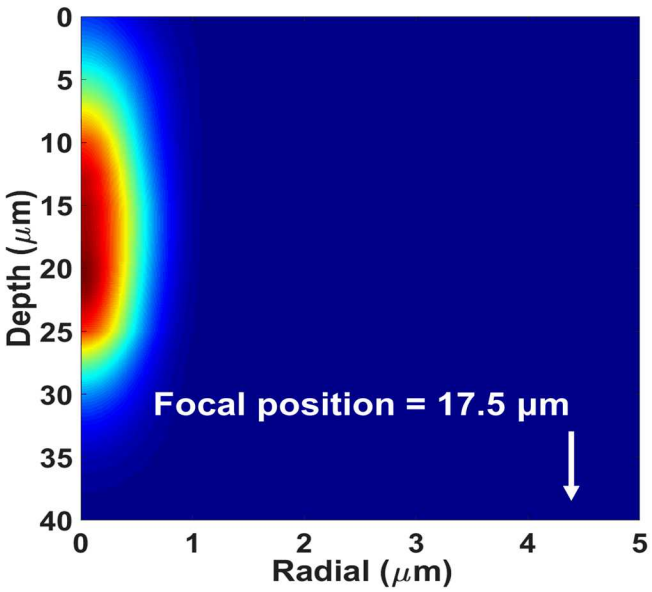

Fig. 1. Time-integrated charge distribution output from Lumerical for a pulse energy of 990 pJ, at a focal position of 17.5 μm. The white arrow shows the direction of pulse propagation.

that done in [9]. The output from Lumerical is a time integrated charge distribution, such as those given in Fig. 2. For each pulse energy and focal position a Lumerical charge distribution was generated and ported into Sentaurus TCAD for charge transport simulations. Comparisons between the experimental results and Lumerical-integrated TCAD simulations can be seen in Fig. 3 (red circles and black squares, respectively) and show good agreement. This verifies that the Lumerical-generated charge distributions are good representations of the physical experiment.

A sensitive volume was defined based on the experimental collected charge from laser-induced single-event transients (SETs) and time integrated charge density profiles from Lumerical. This laser-based sensitive volume was developed assuming: 1) a single sensitive volume with 100% collection efficiency, the volume is radially symmetric and spans the entire device area, 2) charge collection starts at the surface of the device. These assumptions were informed by TCAD simulations and device layout. Equation 1 is the mathematical expression for the sensitive volume defined here, where SV_{laser} is the sensitive volume depth of interest, Q_{coll} is the collected charge, $Q_{gen}(V)$ is the charge generated, V is volume, and A is surface area.

$$Q_{coll} = \iiint_{V=A\,SV_{laser}} \frac{dQ_{gen}(V)}{dV} dV \quad (1)$$

A sensitive volume for each bias condition was found using Eq. 1 with the collected charge and Lumerical charge

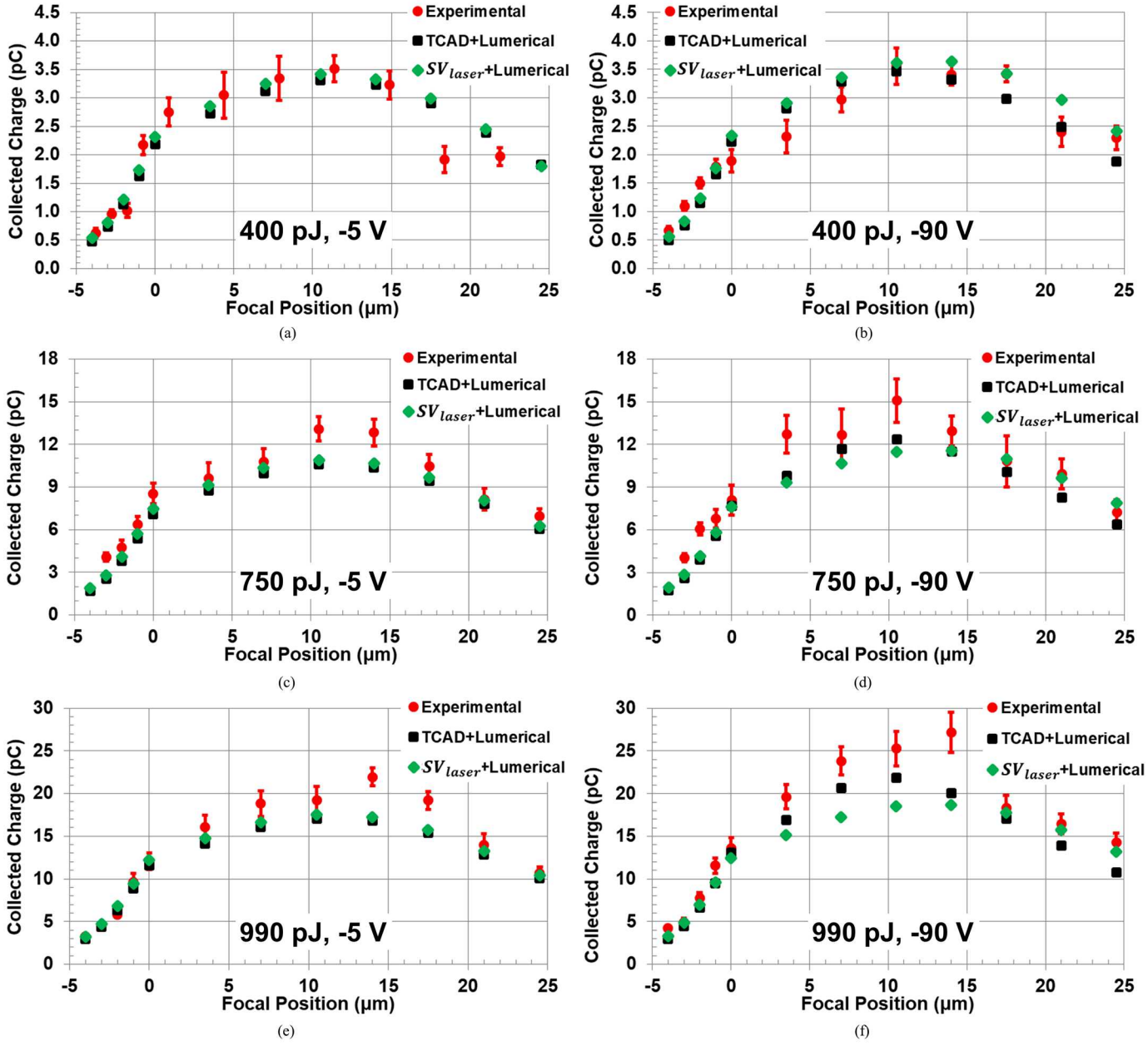

Fig. 3. Collected charge results for a pulse energy of 400 pJ and a bias of (A) -5 V and (b) -90 V, a pulse energy of 750 pJ and a bias of (c) -5 V and (d) -90 V, and a pulse energy of 990 pJ and a bias of (e) -5 V and (f) -90 V. Experimental results are shown as red circles; the error bars represent one standard deviation given 200 SETs. Lumerical-integrated TCAD results are shown as black triangles and laser-based sensitive volume predictions are shows as green diamonds. Both the TCAD and sensitive volume predicts show good agreement with experimental results across all three pulse energies and two biases.

distributions from the 24 µm position at 990 pJ. This particular dataset was chosen because it represents the most extreme of the possible conditions: 24 µm has the most deeply penetrating charge distribution and a pulse energy of 990 pJ is the mostly likely to show nonlinear effects outside of TPA. Sensitive volumes of 23 µm and 26 µm were found for -5 V and -90 V, respectively. The collected charge for each of the other focal positions was predicted by integrating their Lumerical charge distributions over the sensitive volumes found, also shown in Fig. 3 (green diamonds). Overall, there is good agreement between experimental, Lumerical-integrated TCAD, and sensitive volume prediction collected charges across all three pulse energies and both biases. This demonstrates that it is possible to define a single sensitive volume for this diode that well characterizes collected charge for a variety of charge distributions and pulse energies.

IV. Ion-Induced Collected Charge Results

A sensitive volume based on ion-induced collected charge was determined using a similar method to the laser-based sensitive volume by integrating ion LET curves from SRIM [21] to find the path length necessary to get the experimental collected charge. This is expressed mathematically in Eq. 2, in which SV_{ion} is the sensitive volume depth of interest, Q_{coll} is the collected charge, $LET(x)$ is the LET curve, ρ is material density (2320 mg/cm^3 for Si), E_{ehp} is the electron-hole pair creation energy (3.6 eV/ehp in Si), and q is the elementary charge.

$$Q_{coll} = \frac{q\,\rho}{E_{ehp}} \int_0^{SV_{ion}} LET(x)dx \qquad (2)$$

An ion-based sensitive volume for each bias condition was determined by finding a sensitive volume for each ion and then taking the average of the three sensitive volumes to get a single volume for each bias. The average was used to account for possible beam contamination and noise in the measurements. Sensitive volume depths of 15 µm and 25 µm were found for -5 V and -90 V biases, respectively.

Both the ion- and laser-based sensitive volumes were used to find predicted collected charge for each of the ions by integrating the LET curves over the bias-appropriate sensitive volumes. Fig. 4 shows the ion- and laser-based sensitive volume predictions compared to the experimental results (blue triangles, green diamonds, and red circles, respectively). The ion-based sensitive volume shows reasonable agreement with the experimental results, within 12% for both biases. The laser-based sensitive volume, however, over predicts the collected charge at -5 V by between 40-75%. There is good agreement between the laser-based sensitive volume prediction and the experimental results at -90 V.

V. Comparison of Sensitive Volumes

A visual comparison of the ion- and laser-based sensitive volumes and the depletion width at the two biases is shown in Fig. 5. The depletion width was found mathematically using the depletion approximation and then verified using TCAD. At -5 V the device is barely depleted with about 15 µm in the epi-layer for potential modulation to occur before interactions with the heavily doped substrate occur. It is at this condition that the ion- and laser-based sensitive volumes differ the most, with an 8 µm difference. The sensitive volumes at -90 V are nearly identical when the device is almost fully depleted with only 4 µm of epi-layer in which potential modulation can occur. This suggests that the differences in sensitive volume seen at -5 V are due to differences in potential modulation between the ion and laser that get truncated by the substrate when the device is more fully depleted.

Finally, both sensitive volumes were input to CRÈME96 and an error rate was found. The error rate assumed an ISS orbit with solar minimum and quiet magnetosphere conditions (current solar conditions), and a critical charge of 0.5 pC (minimum collected charge experimentally observed). This resulted in an error rate of 2.3×10^{-4} SEEs/bit/second for the ion-based sensitive volume and 4.9×10^{-4} SEEs/bit/second for the laser-based volume. The laser-based sensitive volume results in an error rate over twice as large as the ion-based sensitive volume.

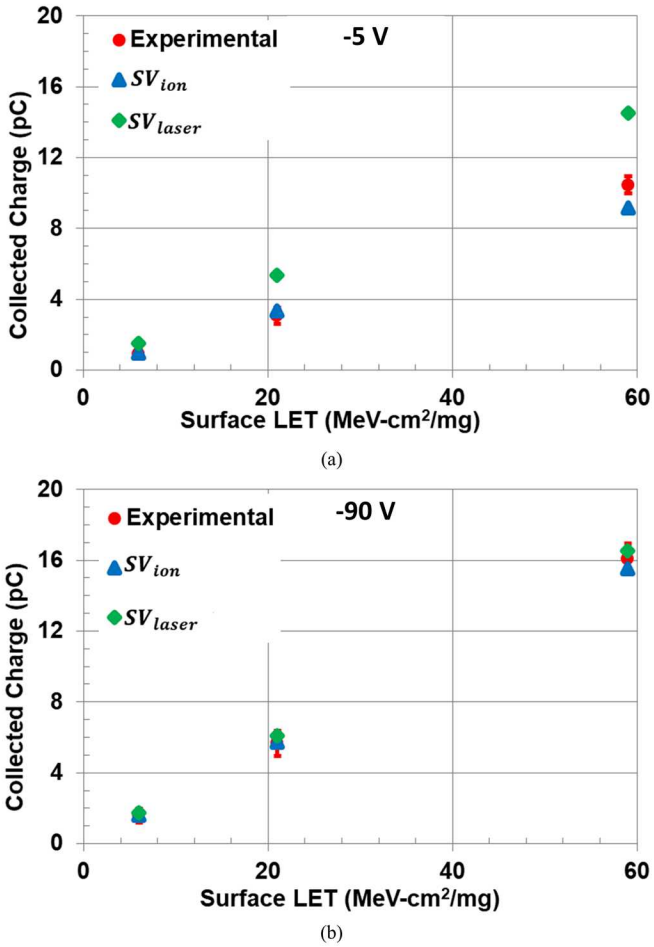

Fig. 4. Ion-induced collected charge results for (a) -5 V bias and (b) -90 V bias. Experimental results are shown as red circles; the error bars represent one standard deviation given 10,000 SETs. Laser-based sensitive volume predictions are shows as green triangles and ion-based sensitive volumes are shown as blue triangles. The ion-based sensitive volume predictions show good agreement with experimental results at both biases, while the laser-based sensitive volume differs from experimental results at -5 V and agrees at -90 V.

VI. Conclusion

Ion- and pulsed laser-induced collected charge experiments were used to define sensitive volumes for an epi-layer silicon diode at two bias conditions. The single laser-based sensitive volume well describes the collected charge results from the laser experiments at multiple pulse energies and focal positions, whereas the laser-based sensitive volume agrees with ion experimental results only at biases when the device is fully depleted. When the device is not fully depleted, differences in potential modulation between the ion- and laser-induced charge cause the respective sensitive volumes to differ.

The differences in the sensitive volumes describing ion- and laser-induced collected charge has implications for error rate calculations, one of the main uses for sensitive volumes. The ion- and laser-based sensitive volumes from -5 V were input to CRÈME96, and the laser-based sensitive volume results in an error rate that is over twice as large as the ion-based sensitive volume. Using the laser-based sensitive volume to predict ion-induced SEEs at -5 V results in an over prediction of collected charge and error rate, while at -90 V the predictions agree with experimental results.

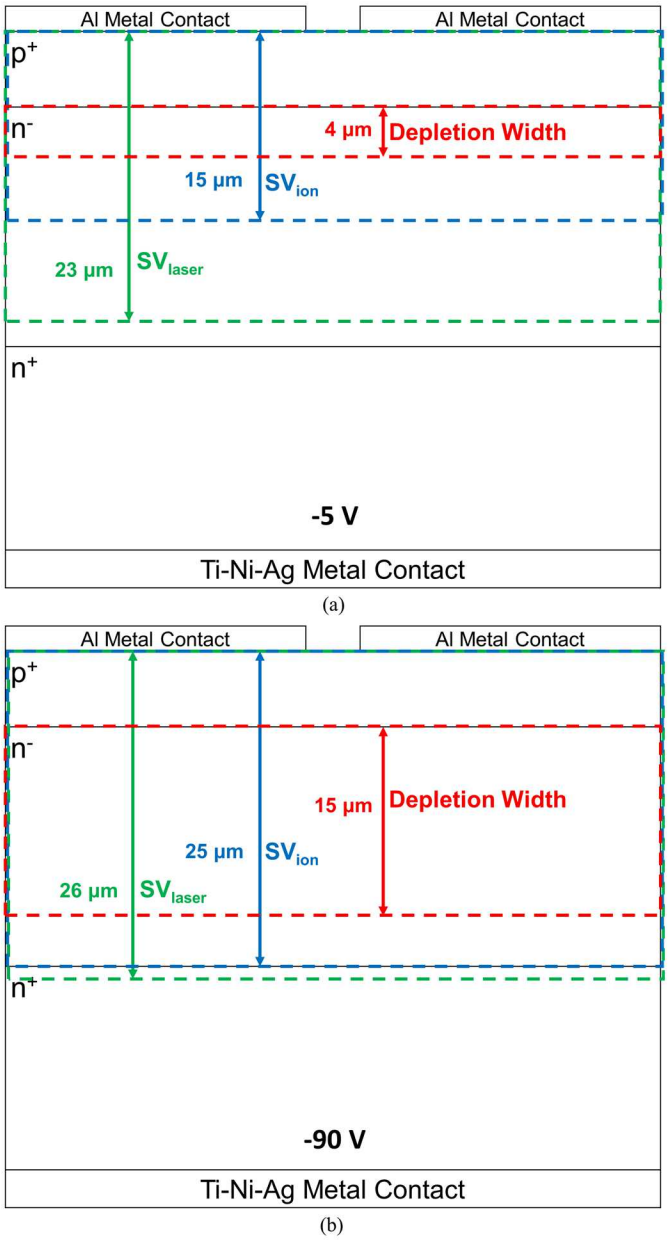

Fig. 5. Comparison for the ion- and laser-based sensitive volumes with the depletion width at (a) -5 V and (b) -90 V. At -5 V the diode is only slightly depleted and so there is 15 µm of epi-later for potential modulation to occur. At -90 V the diode is almost fully depleted and potential modulation will be truncated by the substrate after only 4 µm. The sensitive volumes differ when potential modulation is not truncated by the substrate.

Acknowledgement

The authors would like to thank DTRA's basic research program for their general support and Sandia National Lab's LDRD program for their graduate student and travel support.

References

[1] J. C. Pickel and J. T. Blandford Jr., "Cosmic ray induced errors in MOS memory cells," *IEEE Trans. Nucl. Sci.*, vol. NS-25, p. 1166, 1978.

[2] E. L. Petersen, "Predictions and observations of SEU rates in space," *IEEE Trans. Nucl. Sci.*, vol. 44, p. 2174, 1997.

[3] B. D. Sierawski, J. A. Pellish, R. A. Reed, R. D. Schrimpf, K. M. Warren, R. A. Weller, M. H. Mendenhall, J. D. Black, A. D. Tipton, M. A. Xapsos, R. C. Baumann, X. Deng, M. J. Campola, M. R. Friendlich, H. S. Kim, A. M. Phan, and C. M. Seidleck, "Impact of Low-Energy Proton Induced Upsets on Test Methods and Rate Predictions," *IEEE Trans. Nucl. Sci.*, vol. 56, pp. 3085-3092, Dec. 2009.

[4] K. M. Warren, R. A. Weller, B. D. Sierawski, R. A. Reed, M. H. Mendenhall, R. D. Schrimpf, L. W. Massengill, M. E. Porter, J. D. Wilkinson, K. A. LaBel, and J. H. Adams, "Application of RADSAFE to Model the Single Event Upset Response of a 0.25 um CMOS SRAM," *IEEE Trans. Nucl. Sci.*, vol. 54, pp. 898-903, Aug. 2007.

[5] A. J. Tylka, J. H. Adams, Jr., P. R. Boberg, B. Brownstein, W. F. Dietrich, E. O. Flueckiger, E. L. Petersen, M. A. Shea, D. F. Smart, and E. C. Smith, "CREME96: A Revision of the Cosmic Ray Effects on Micro-Electtronics Code," *IEEE Trans. Nucl. Sci.*, vol. 4, pp. 2150-2160, Dec. 1997.

[6] Marcus H. Mendenhall and Robert A. Weller, "A probability-conserving cross-section biasing mechanism for variance reduction in Monte Carlo particle transport calculations", *Nucl. Inst. & Meth. A*, Volume 667, 1 March 2012, Pages 38-43, doi:10.1016/j.nima.2

[7] R. A. Weller, M. H. Mendenhall, R. A. Reed, R. D. Schrimpf, K. M. Warren, B. D. Sierawski, and L. W. Massengill, "Monte carlo simulation of single event effects," *IEEE Trans. Nucl. Sci.*, vol. 57, no. 4, pp. 1726-1746, Aug. 2010.

[8] D. McMorrow, W. T. Lotshaw, J. S. Melinger, S. Buchner, Y. Boulghassoul, L. W. Massengill, and R. L. Pease, "Three-Dimensional Mapping of Single-Event Effects Using Two Photon Absorption," *IEEE Trans. Nucl. Sci.*, vol. 50, pp. 2199-2207, Dec. 2003."

[9] S. P. Buchner, F. Miller, V. Pouget, and D. P. McMorrow, "Pulsed-Laser Testing for Single-Event Effects Investigations," *IEEE Trans. Nucl. Sci.*, vol. 60, pp. 1852-1875, June 2013.

[10] J. M. Hales, A. Khachatrian, N. J. Roche, J. H. Warner, S. P. Buchner, and D. McMorrow, "Simulation of Laser-Based Two-Photon Absorption Induced Charge Carrier Generation in Silicon,"

IEEE Trans. Nucl. Sci., vol. 62, pp. 1550-1557, Aug. 2015.

[11] J. M. Hales, N. J. Roche, A. Khachatrian, D. McMorrow, S. Buchner, J. Warner, M. Turowski, K. Lilja, N. C. Hooten, E. Zhang, R. A. Reed, R. D. Schrimpf, "Strong Correlation Between Experiment and Simulation for Two-Photon Absorption Induced Carrier Generation," *IEEE Trans. Nucl. Sci.*, vol. 64, pp. 1133-1136, May 2017.

[12] Z. E. Fleetwood, N. E. Lourenco, A. Ildefonso, J. H. Warner, M. T. Wachter, J. M. Hales, G. N. Tzintzarov, N. J. Roche, A. Khachatrian, S. P. Buchner, D. McMorrow, P. Paki, and J. D. Cressler, "Using TCAD Modeling to Compare Heavy-Ion and Laser-Induced Single Event Transients in SiGe HBTs," *IEEE Trans. Nucl. Sci.*, vol. 64, pp. 398-405, Jan. 2017.

[13] A. Ildefonso, Z. E. Fleetwood, G. N. Tzintzarov, J. M. Hales, D. Nergui, M. Froumchi, A. Khachatrian, S. P. Buchner, D. McMorrow, J. H. Warner, J. Harms, A. Erickson, K. Voss, V. Ferlet-Cavrois, and J. D. Cressler, "Optimizing Optical Parameters to Facilitate Correlation of Laser- and Heavy-Ion-Induced Single-Event Transients in SiGe HBTs," *IEEE Trans. Nucl. Sci.*, vol. 66, pp. 359-367, Jan. 2019.

[14] J. M. Hales, A. Khachatrian, S. Bucnher, N. J. Roche, J. Warner, Z. E. Fleetwood, A. Ildefonso, J. D. Cressler, V. Ferlet-Cavrois, and D. McMorrow, "Experimental Validation of an Equivalent LET Approach for Correlating Heavy-Ion and Laser-Induced Charge Deposition," *IEEE Trans. Nucl. Sci.*, vol. 65, pp. 1724-1733, Aug. 2018.

[15] I. K. Samsel, E. Zhang, N. C. Hotten, E. D. Funkhouser, W. G. Bennett, R. A. Reed, R. D. Schrimpf, M. W. McCurdy, D. M. Fleetwoood, R. A. Weller, G. Vizkelethy, X. Sun, T. Ma, O. I. Saadat, and T. Palacios, "Charge Collection Mechanisms in AlGaN/GaN Mos High Electron Mobility Transistors," *IEEE Trans. Nucl. Sci.*, vol. 60, pp. 4439-4445, Dec. 2013.

[16] J. A. Pellish, R. A. Reed, D. McMorrow, G. Vizkelethy, V. F. Cavrois, J. Baggio, P. Paillet, O. Duhamel, K. A. Moen, S. D. Phillips, R. M. Diestelhorst, J. D. Cressler, A. K. Sutton, A. Raman, M. Turowski, P. E Dodd, M. L. Alles, R. D. Schrimpf, P. W. Marshall, and K. A. Label, “Heavy ion microbeam- and broadbeam-induced transients in SiGe HBTs,” *IEEE Trans. Nucl. Sci.*, vol. 56, no. 6, pp. 3078–3084, Dec. 2009.

[17] M. B. Johnson. Cocktails and Ions [Online]. Available FTP: http://cyclotron.lbl.gov/

[18] A. Khachatrian, N. J. Roche, D. McMorrow, J. H. Warner, S. P. Buchner, and J. S. Melinger, “A Dosimetry Methodology for Two-Photon Absorption Induced Single-Event Effects Measurements,” *IEEE Trans. Nucl. Sci.*, vol. 61, pp. 3416-3423, Dec. 2014.

[19] Lumerical. FDTD Solutions. Accessed: Apr. 2017. [Online]. Available: https://www.lumerical.com/tcad-products/fdtd/

[20] L. D. Ryder et. al., "A First Principles Simulation Approach of Pulsed Laser Induced Single Event Effect Transients," To be published.

[21] J. F. Ziegler, SRIM - The Stopping and Range of Ions in Matter.